# Synaptic activity becomes excitotoxic in neurons exposed to elevated levels of platelet-activating factor

Matthew J. Bellizzi,[1] Shao-Ming Lu,[1] Eliezer Masliah,[2] and Harris A. Gelbard[1,3]

[1]Department of Neurology, Child Neurology Division, Center for Aging and Developmental Biology, University of Rochester School of Medicine and Dentistry, Rochester, New York, USA. [2]Department of Neurosciences and Department of Pathology, School of Medicine, University of California San Diego, La Jolla, California, USA. [3]Departments of Pediatrics and Microbiology and Immunology, University of Rochester School of Medicine and Dentistry, Rochester, New York, USA.

**Neurologic impairment in HIV-1–associated dementia (HAD) and other neuroinflammatory diseases correlates with injury to dendrites and synapses, but how such injury occurs is not known. We hypothesized that neuroinflammation makes dendrites susceptible to excitotoxic injury following synaptic activity. We report that platelet-activating factor, an inflammatory phospholipid that mediates synaptic plasticity and neurotoxicity and is dramatically elevated in the brain during HAD, promotes dendrite injury following elevated synaptic activity and can replicate HIV-1–associated dendritic pathology. In hippocampal slices exposed to a stable platelet-activating factor analogue, tetanic stimulation that normally induces long-term synaptic potentiation instead promoted development of calcium- and caspase-dependent dendritic beading. Chemical preconditioning with diazoxide, a mitochondrial ATP-sensitive potassium channel agonist, prevented dendritic beading and restored long-term potentiation. In contrast to models invoking excessive glutamate release, these results suggest that physiologic synaptic activity may trigger excitotoxic dendritic injury during chronic neuroinflammation. Furthermore, preconditioning may represent a novel therapeutic strategy for preventing excitotoxic injury while preserving physiologic plasticity.**

## Introduction

Neurologic impairment in patients with HIV-1–associated dementia (HAD) correlates well with injury to dendrites and synapses (1) but poorly with neuronal loss (2, 3). Similar results have been found in Alzheimer disease (4, 5), and dendritic injury in both diseases is characterized by focal swelling or beading, loss of spines, and reductions in overall dendritic and synaptic areas (6–9). Consequently, synaptic protection represents an area of considerable therapeutic interest.

Dendrites can undergo extensive localized damage even when the neuron survives (10–13) but have a remarkable capacity for recovery. In vitro exposure to sublethal excitotoxic stimuli can cause dendritic beading (10, 14, 15), retraction of spines (16), and loss of synaptic transmission (17) that can all recover after washout of the excitotoxin. Beaded neurites can recover in vivo following β-amyloid clearance in a murine model for Alzheimer disease (18), and dendritic beading and recovery parallel the onset and remission of reversible neurologic deficits in experimental autoimmune encephalitis (19) and a model for noise-induced hearing loss (20). Thus, dendrite injury may underlie the significant reversible component of HAD (21, 22) and may underlie a potential for reversibility in other neurodegenerative diseases.

How HIV-1 causes dendritic injury is not well understood. HIV-1 infects neurons rarely, if at all, but predominantly infects macrophages and microglia in the brain and triggers release of inflammatory mediators including HIV-1 Tat and gp120, proinflammatory cytokines, arachidonic acid metabolites, and platelet-activating factor (PAF) (23). These functionally-diverse toxins appear to act on neurons via pathways that converge on elevated PAF signaling (24) and subsequent N-methyl-D-aspartate (NMDA) receptor-mediated excitotoxicity (25).

PAF (1-O-alkyl-2-O-acetyl-sn-glycero-3-phosphocholine) is a phospholipid inflammatory mediator that plays both physiologic and pathologic roles in the brain. Produced by neurons in response to NMDA receptor activation (26), PAF increases glutamate release from presynaptic terminals (27) and can participate in long-term potentiation (LTP) of synaptic transmission (28, 29) as well as learning and memory (30, 31). PAF brain concentrations are dramatically increased in HAD (32) and other insults (33, 34) and are associated with neurotoxicity. PAF has been shown to mediate NMDA excitotoxicity (35), and high concentrations can kill neurons in an NMDA receptor–dependent manner (32, 36).

Because PAF can augment excitatory synaptic transmission as well as promote excitotoxicity, we hypothesized that elevated levels of PAF in HAD would increase neuronal vulnerability to excitotoxic dendritic injury following elevated synaptic activity. Here we report that carbamyl PAF (cPAF), a nonhydrolyzable PAF analog chosen because PAF is rapidly inactivated by tissue acetylhydrolases (37), promoted dendritic beading and failure of LTP in a calcium- and caspase-dependent manner following high-frequency synaptic stimulation in hippocampal slices. Pretreatment with the mitochondrial ATP-sensitive potassium channel (K$_{ATP}$) agonist
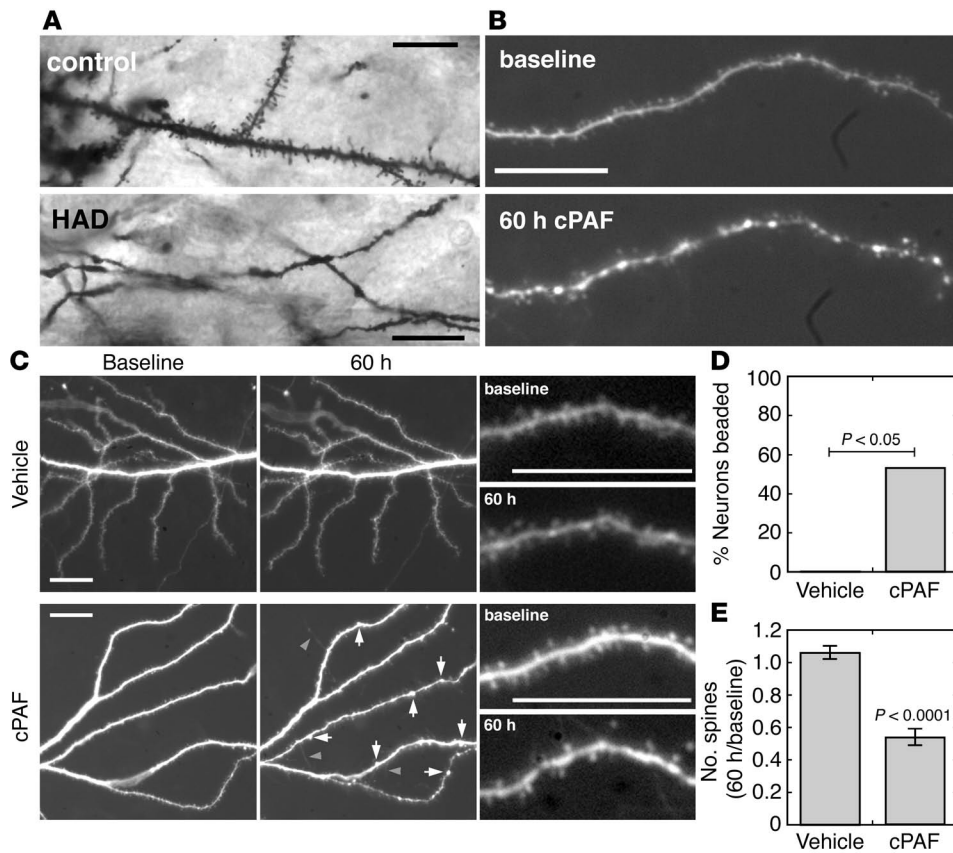
**Figure 1**
cPAF reproduces dendritic pathology of HAD. (**A**) Golgi-stained neurons in brain tissue from patients with HAD show focal swellings and fewer dendritic spines than those from HIV-1 seropositive controls without neurologic disease. (**B**) Dendrites in dissociated hippocampal cultures developed similar focal swellings and decreased numbers of spines after prolonged exposure to cPAF. (**C**) Lower-magnification images (left, middle columns) show dendritic beading (arrows) accompanied by sprouting of filopodia (arrowheads) with preservation of dendrite branches in cPAF-treated cultures and minimal change in dendrite morphology in vehicle-treated cultures. Higher-power images from the same cells (right column) show dendritic spine numbers maintained in a control dendrite and loss of spines in a cPAF-treated dendrite. (**D**) Of cPAF-treated neurons, 56% developed dendritic beading while none of the vehicle-treated cells did ($n = 17$, $P < 0.05$). (**E**) Numbers of dendritic spines decreased by 45% ± 5% with cPAF treatment and remained stable in control neurons ($n = 10$, $P < 0.0001$). Scale bars: 20 μm.

Dendrites in dissociated hippocampal cultures developed nearly identical pathology during a 60-hour exposure to a sublethal (130 nM) dose of cPAF (Figure 1B). We studied hippocampal neurons in vitro because hippocampal dendrites are injured in HAD (6) and PAF effects on synaptic function and excitotoxicity have been well studied in these model systems. We transfected neurons in 3- to 4-week-old cultures with red or yellow fluorescent proteins (mRFP or EYFP) and compared images of the same cells taken before and after cPAF exposure. While dendritic arbors remained grossly intact, maintaining similar branching and projection patterns (Figure 1C), cPAF exposure led to dendritic beading and loss of dendritic spines. Small focal swellings developed along dendritic shafts in 56% of serially imaged cPAF-exposed cells while no beading developed in control cells (Figure 1D, $n = 17$ cells from 4 cultures; $P < 0.05$). Numbers of dendritic spines remained stable in control cells (6.2% ± 4.1% increase over 60 hours) but decreased by 45.1% ± 5.0% with cPAF exposure (Figure 1E, $n = 10$ cells from 4 cultures; $P < 0.0001$). Most spines in these cultures were short and mushroom shaped at baseline, but disruption of mature spines in cPAF-treated cells was often accompanied by the appearance of longer spines and filopodia (Figure 1, B and C). Treatment with 130 nM cPAF did

diazoxide prevented beading and restored LTP. We propose that during HIV-1 infection of the brain, elevated PAF signaling may put neurons at risk for activity-dependent dendritic injury, thereby disrupting synaptic function. This has significant implications for the understanding and treatment of HAD.

## Results

*cPAF exposure leads to dendritic beading and spine loss.* Because in vitro studies have implicated PAF as a common downstream mediator for the actions of diverse neurotoxins in HAD (24), we tested whether exposure to elevated PAF signaling can recapitulate the dendritic injury seen in HAD. Golgi-stained cortical neurons in tissue from patients with HAD ($n = 5$) showed focal swellings, or beading, and very few spines, while those in tissue from HIV-1 seropositive patients without neurologic disease ($n = 5$) had many spines and no beading (Figure 1A). This is consistent with previous studies of HAD neuropathology (7).

not lead to death of any of the cells that we imaged or decrease overall neuronal survival in cultures as assessed by Hoechst and propidium iodide staining (80.2% ± 4.3% cPAF vs. 79.0% ± 2.3% vehicle control, $n = 3$ cultures; $P = 0.77$).

Immunohistochemical staining from cortical tissue from patients with HAD and dendritic injury (Figure 2A) demonstrated increased expression of PAF receptor (PAF-R) on neuronal cell bodies and dendrites compared with HIV-1 seropositive controls (Figure 2, B and C). Coimmunostaining for microtubule-associated protein-2 (MAP2), a marker for dendrites and neuronal cell bodies, showed PAF-R expression on nearly all dendrites in both HAD and control tissue. Nonneuronal cells expressing PAF-R were also present in both conditions, consistent with previous studies (38), and PAF-R staining was eliminated by preincubation with a PAF-R–derived peptide antigen (Supplemental Figure 1; supplemental material available online with this article; doi:10.1172/JCI25444DS1), corroborating the specificity of PAF-R
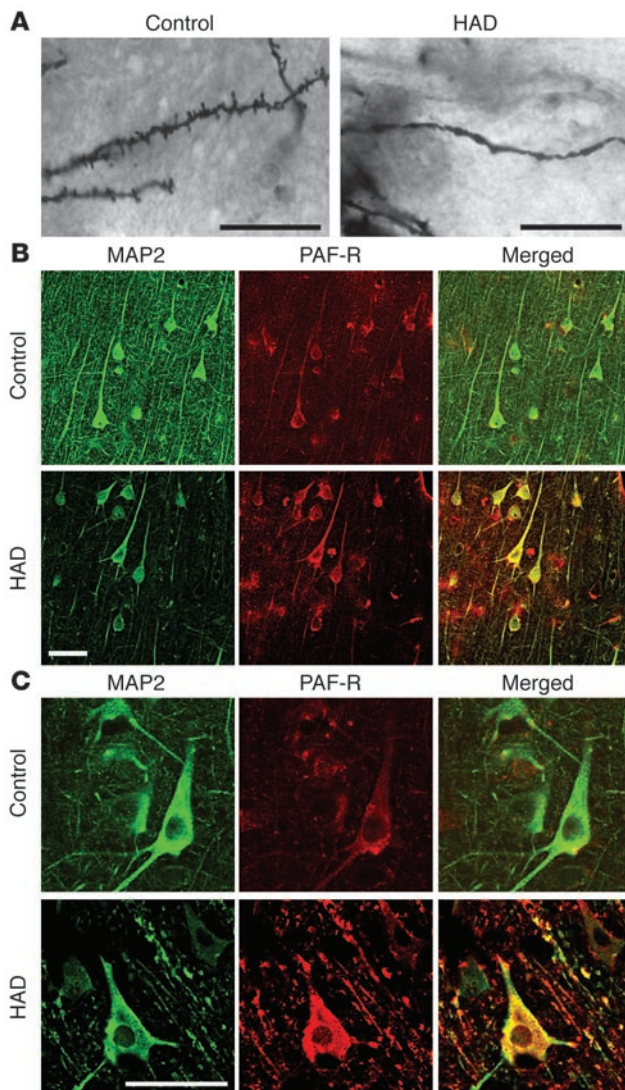
**Figure 2**
Dendritic injury and neuronal PAF-R expression in HAD. In cortical tissue from patients with HAD (**A**), dendritic beading and spine loss in Golgi-stained neurons is associated with (**B**) strong PAF-R immunohistochemical staining on dendrites and neuronal cell bodies identified by coimmunostaining for MAP2. HAD tissue shows fewer MAP2-positive dendritic branches compared with tissue from HIV-1 seropositive controls while PAF-R expression on the remaining dendrites and cell bodies is increased. (**C**) Higher-power field shows intense PAF-R expression on beaded dendrites in HAD compared with control dendrites. Scale bars: 20 μm.

following 5-second pulses that evoked stronger and more prolonged depolarization (Figure 3C). Acute (20 to 90 minutes) exposure to 130 nM cPAF lowered the threshold for dendritic beading so that 90% of imaged cells beaded in response to 3 1-second KCl pulses (Figure 3, B and D, $n = 40$ cells from 9 cultures; $P < 0.0001$ vs. control). Beading was prevented by glutamate receptor antagonists CNQX (10 μM) and AP-5 (50 μM) (1-second KCl pulses, $n = 42$ cells from 9 cultures; $P < 0.0001$ vs. cPAF), indicating that it resulted from KCl-induced glutamate release and not from depolarization alone.

Increased vulnerability of cPAF-exposed dendrites was blocked by pretreatment with the PAF-R antagonist BN52021 (10 μM); no cells developed beading after 1-second KCl pulses ($n = 38$ cells from 9 cultures; $P < 0.0001$ vs. cPAF alone), and 86% beaded after 5-second pulses (Figure 3D), similar to controls. Beading in both cPAF- and vehicle-exposed cultures developed rapidly (appearing within 10 seconds of the stimulus), began to recover within 1 to 2 minutes, and was fully resolved after 5 to 10 minutes in all imaged cells. Rapid recovery of KCl-induced beading was prevented by application of 5-nitro-2-(3-phenyl-propylamino) benzoic acid (NPPB) (100 μM) (Figure 3E, $n = 6$ cells), a Cl⁻ channel blocker that inhibits volume-sensitive anion channels opened in response to neuronal swelling (40). This suggests that KCl-induced beading reflects acute dendritic swelling without lasting excitotoxicity.

*cPAF promotes dendritic beading and failure of LTP in hippocampal slices.* We next tested whether cPAF might disrupt synaptic plasticity by increasing vulnerability to activity-dependent dendritic injury in hippocampal slices. We measured dendritic beading and potentiation of excitatory postsynaptic potentials (EPSPs) in individual CA1 pyramidal cells in acute rat hippocampal slices following high-frequency stimulation (HFS) of Schaffer collateral afferents. We recorded EPSPs by whole-cell patch clamp and injected Alexa Fluor 568 hydrazide via the recording pipette for simultaneous dendrite imaging. In slice experiments, we used a higher (1 μM) dose of cPAF that, consistent with previous studies (27, 29), was sufficient to augment excitatory transmission (data not shown) but was nontoxic to neurons in our slices; exposure to 1 μM cPAF for up to 7 hours did not affect baseline membrane potential (–63 ± 3.6 mV cPAF, $n = 57$ cells, vs. –63 ± 3.4 mV vehicle, $n = 39$ cells; $P = 0.99$) or the ability to fire action potentials.

In control slices, HFS (3 1-second pulses, 100 Hz trains, 20 seconds apart) elicited a robust, long-lasting potentiation of excitatory synaptic transmission (Figure 4D); the rising slope of the postsynaptic potential increased 2.5-fold over baseline values following HFS (2.66 ± 0.44 from 40 to 50 minutes, $n = 13$ slices from 13 animals; $P < 0.001$) and showed no decrement for

immunohistochemistry in this tissue. While MAP2-positive dendrites were markedly reduced in HAD, as reported previously (1), PAF-R expression appeared to be increased on remaining dendrites and cell bodies and was dramatically increased on beaded dendrites (Figure 2C) compared with controls. The widespread dendritic expression of PAF-R is consistent with a role for PAF in synaptic plasticity and excitotoxic injury. In addition to elevations in brain PAF concentration (32), increased PAF-R expression may further contribute to dendritic vulnerability in HAD.

*cPAF increases vulnerability to rapid dendritic beading following elevated synaptic activity.* Next we asked whether cPAF increases dendrites' vulnerability to injury from synaptic activity. Because modulating spontaneous activity for 60 hours altered dendrite morphology in preliminary experiments and confounded cPAF effects (data not shown), we tested this by measuring dendritic beading in cultured neurons after stimulating acute neurotransmitter release via depolarizing pulses of KCl. Control neurons showed no change in dendrite morphology following 3 1-second pulses of KCl, a stimulus that causes NMDA receptor-dependent synaptic potentiation in dissociated cultures (39), but rapidly developed beading throughout their dendritic arbors (Figure 3A)
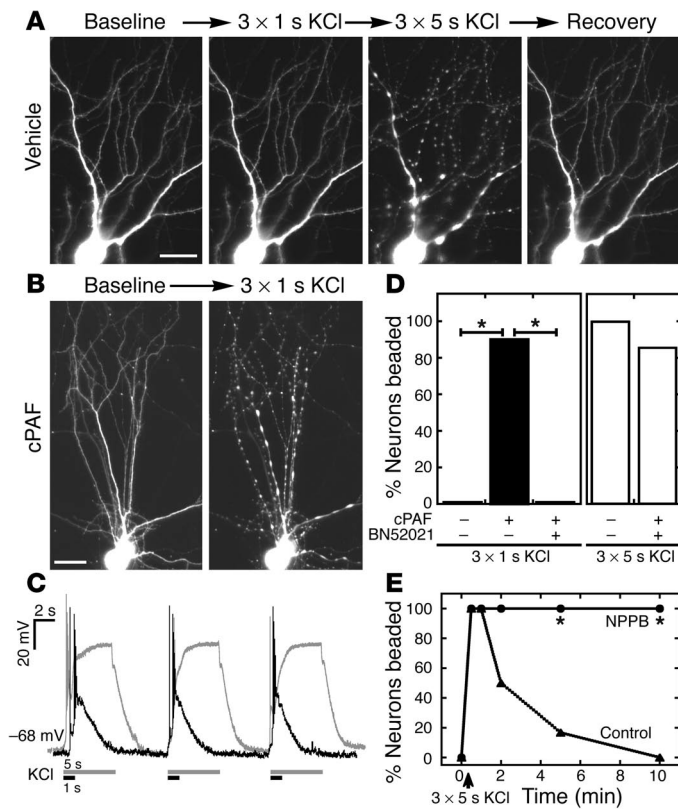
**Figure 3**
cPAF increases vulnerability to dendritic swelling following synaptic activity. (**A**) In control cultures, synaptic activity due to 1-second depolarizing pulses of KCl elicited no change in dendrite morphology while 5-second pulses triggered beading throughout the dendritic arbor, which recovered within 10 minutes. (**B**) In cPAF-exposed cells, 1-second pulses caused rapid dendritic beading. (**C**) Membrane potential recordings show bursts of action potentials and stronger, more prolonged depolarization elicited by 5-second (white) versus 1-second (black) KCl stimulation. (**D**) cPAF lowered the threshold for activity-induced dendritic beading, leading to beading in 90% of neurons following 1-second KCl pulses that caused no beading in control neurons. PAF-R antagonist BN52021 blocked the increase in vulnerability. (**E**) Rapid recovery of dendritic beading is prevented by NPPB, an inhibitor of regulatory volume decrease in swollen neurons. *$P < 0.001$. Scale bars: 20 μm.

the duration of the recording period (50 minutes). No vehicle-treated cells developed dendritic beading or other apparent changes in dendrite morphology during the recording session (Figure 4, A and B).

In contrast, exposure to 1 μM cPAF for 20 to 60 minutes prior to the recording session led to dendritic beading following HFS in 57% of recorded neurons (Figure 4, A and B, $n = 19$ slices from 17 animals; $P < 0.001$ vs. vehicle). HFS-induced dendritic beading was associated with a failure of synaptic potentiation (Figure 4D): cPAF-exposed neurons that beaded showed no potentiation of EPSPs following HFS ($0.84 \pm 0.12$ relative to baseline from 40 to 50 minutes, $n = 11$; $P < 0.01$ vs. vehicle). On the other hand, cPAF-exposed cells that did not develop dendritic beading did undergo a long-lasting potentiation ($1.60 \pm 0.26$ relative to baseline from 40 to 50 minutes, $n = 8$; $P < 0.05$) although of a smaller magnitude than vehicle-treated cells. While exogenous PAF application has been proposed to occlude LTP in some experi-

mental paradigms (28), this result indicates that 1 μM cPAF at most partially occluded LTP in our experiments. Furthermore, EPSP potentiation was significantly different at all time points after HFS between cPAF-exposed cells that beaded and those that did not ($P < 0.05$), strongly suggesting that failure of potentiation was a result of synaptic injury associated with dendritic beading.

Dendritic beading in cPAF-exposed slices was largely prevented by structurally distinct PAF-R antagonists (Figure 4B); rates of beading following HFS in cPAF-exposed neurons were reduced to 14% by coapplication of PAF analog CV-3988 (10 μM; $n = 7$ slices from 3 animals; $P < 0.05$ vs. cPAF alone) and to 10% by the structurally unrelated antagonist BN52021 (2 μM; $n = 10$ slices from 5 animals; $P < 0.05$ vs. cPAF alone). PAF-R antagonists did not restore LTP in cPAF-exposed slices (Supplemental Figure 2); EPSP recordings demonstrated a small potentiation in BN52021-treated slices ($1.29 \pm 0.05$ relative to baseline from 40 to 50 minutes; $P < 0.05$) and no significant potentiation in CV-3988–treated slices ($1.07 \pm 0.13$ relative to baseline from 40 to 50 minutes; $P = 0.55$).

cPAF-exposed neurons were depolarized for similar durations ($693 \pm 296$ ms cPAF, $n = 22$, vs. $750 \pm 283$ ms vehicle, $n = 15$; $P = 0.56$) and to similar extents ($31.8 \pm 11.9$ mV cPAF vs. $27.8 \pm 5.6$ mV vehicle; $P = 0.19$) as controls during HFS (Figure 4C), suggesting no gross differences in glutamate receptor activation between conditions.

In cPAF-exposed cells, HFS-induced dendritic beading appeared after a delay, typically of 15–35 minutes, and often became more prominent throughout the recording session (Figure 5). Beading developed at discrete locations and did not appear to disrupt dendritic spines in the intervening areas (Figures 4, A and 5). We never observed recovery of HFS-induced beading during the recording sessions (50 to 80 minutes after HFS) though all neurons in the study remained viable throughout, maintaining negative membrane potentials and the ability to fire action potentials that overshot 0 mV. In addition, we did not observe rapid dendritic swelling during or immediately after HFS in any dendrites, and no cells developed beading in the absence of HFS regardless of whether they were exposed to cPAF for up to 5 hours or recorded in whole-cell mode for up to 90 minutes (data not shown).

*Chemical preconditioning prevents calcium- and caspase-dependent dendritic beading.* The delayed, progressive, and long-lasting appearance of beading following HFS led us to suspect a calcium-mediated excitotoxic injury in the dendrites. We tested this by including 5 mM 1,2-bis(2-aminophenoxy)ethane-N,N,N′,N′-tetraacetic acid (BAPTA) in the recording pipette to chelate calcium in the postsynaptic cell of cPAF-exposed slices. BAPTA prevented dendritic beading (Figure 6A, $n = 6$ slices from 2 animals; $P < 0.05$ vs. cPAF alone) and eliminated synaptic potentiation in all cells (Figure 6B). We then tested whether HFS-induced beading requires caspase activation in the postsynaptic cell by intracellular application of N-acetyl-Asp-Glu-Val-Asp aldehyde (Ac-DEVD-CHO) (10 μM), an inhibitor of caspase-3, -6, -7, -8, and -10, via the recording pipette. Caspase inhibition prevented beading following HFS in all cPAF-exposed slices (Figure 6A, $n = 7$ slices from 4 animals; $P < 0.01$ vs. cPAF alone), but failed to rescue LTP. After an initial 2-fold potentiation (Figure 6B, $1.97 \pm 0.28$ relative to baseline from 0 to 10 minutes; $P < 0.01$) the EPSP slope gradually declined until it was not different from baseline at 40 to 50 minutes after HFS
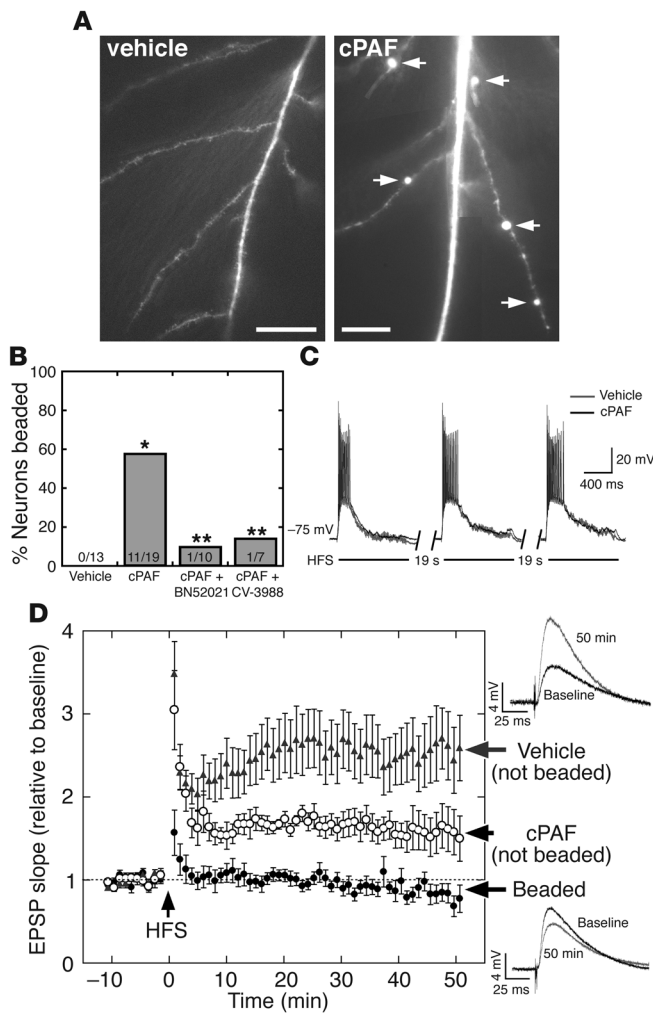
**Figure 4**
cPAF replaces LTP with dendritic beading in hippocampal slices. (**A**) Dendritic beading (arrows) in a cPAF-exposed CA1 pyramidal neuron 45 minutes after high-frequency Schaffer collateral stimulation (HFS) with no disruption of dendrite or spine morphology in following HFS in vehicle-treated cells. (**B**) HFS elicited dendritic beading in 11 of 19 cells from cPAF-treated slices and in 0 of 13 cells from vehicle-treated slices. *$P < 0.001$. PAF-R antagonists BN52021 and CV-3988 reduced dendritic beading to 1 of 10 and 1 of 7 cells, respectively. **$P < 0.05$ vs. cPAF. (**C**) The amplitude and duration of postsynaptic depolarization during HFS is unaffected by cPAF exposure. (**D**) Excitatory synaptic transmission is strongly potentiated following HFS in vehicle-treated slices (2.66 ± 0.44–fold relative to baseline at 40 to 50 minutes, $n = 13$, $P < 0.001$). In cPAF-treated slices, cells that did not develop dendritic beading underwent a smaller but significant potentiation (1.60 ± 0.26 relative to baseline, $n = 8$, $P < 0.05$) while EPSPs in cells whose dendrites did bead were not potentiated at all (0.84 ± 0.12 relative to baseline, $n = 11$, $P < 0.01$ vs. vehicle and $P < 0.05$ vs. cPAF-treated cells without dendritic beading). Representative EPSPs from vehicle-treated (upper right) and beaded cPAF-treated cells (lower right) are averages of 10 consecutive traces recorded at baseline and 50 minutes after HFS. Scale bars: 20 μm.

mimic the dendritic pathology of HAD. This can disrupt synaptic function by promoting calcium- and caspase-dependent dendritic beading and failure of EPSP enhancement following excitatory activity that normally induces LTP. These findings suggest that in the presence of inflammatory mediators, physiologic synaptic activity has the potential to trigger dendritic injury and synaptic dysfunction. Thus, there may be an activity-dependent component to neuronal injury in HAD and perhaps other neurodegenerative diseases.

The time course and spatial distribution of dendritic beading in cPAF-exposed hippocampal slices (Figure 5) suggests a different type of injury than that elicited by bath-applied KCl (Figure 3) or by glutamate receptor agonists in previous studies (14, 15, 17). KCl and bath-applied agonists trigger beading that develops rapidly, affects nearly the entire dendritic arbor, and begins to recover soon after stimulus washout. Rapid, reversible beading has been shown to primarily reflect dendritic swelling driven by large Na$^+$ and Cl$^-$ influxes and independent of calcium entry (14, 15). Consistent with this, we show that NPPB, a Cl$^-$ channel blocker that inhibits volume-sensitive currents crucial for reducing neuronal swelling (40), prevents rapid recovery of KCl-induced beading. In contrast, beading following high-frequency Schaffer collateral stimulation appears to reflect local excitotoxic injury in the dendrites; it is delayed, long-lasting, dependent on postsynaptic calcium and caspase activity, and disrupts discrete dendritic regions while leaving the majority of the arbor intact. We did not see acute dendritic swelling following HFS; though bicuculline in the bath during EPSP recording experiments could have attenuated acute swelling by reducing Cl$^-$ influx (14), similar results were seen in slices stimulated without bicuculline (data not shown).
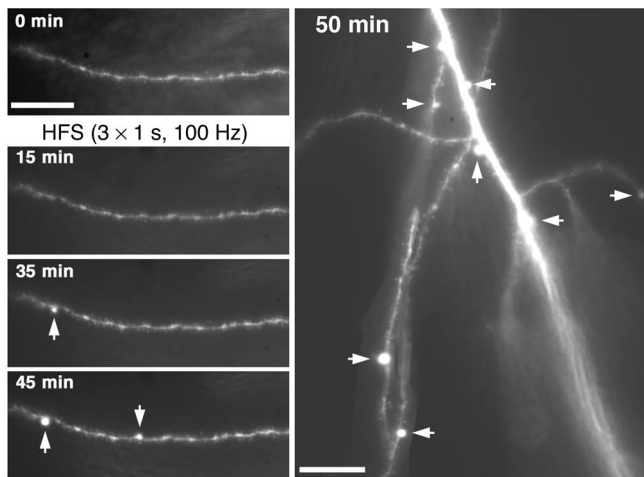
It is likely that activation of a small subset of synapses by Schaffer collateral stimulation, compared with widespread activation by bath-applied stimuli, limits ion influxes and thus avoids acute volume overload in the dendrites. This may have important functional implications. Rapid Na$^+$, Cl$^-$-dependent swelling has been proposed to protect neurons from high levels

(1.22 ± 0.19 relative to baseline; $P > 0.25$). Because PAF has been reported to increase functional coupling between NMDA receptors and neuronal nitric oxide production (41), we tested whether nitric oxide synthase inhibition by L-NAME (100 μM) could prevent beading. This offered no protection compared with treatment with cPAF alone (Figure 4B), with 57% of L-NAME–treated cells (Figure 6A, $n = 7$ slices from 3 animals) beading after HFS.

Finally, because HFS-induced dendritic beading appeared to be calcium and caspase mediated, we tested whether diazoxide, an agonist of K$_{ATP}$ that has been shown to precondition neurons against a variety of excitotoxic insults (42–44), could protect against beading. Pretreatment with bath-applied diazoxide (30 μM) for 40 to 60 minutes prior to HFS in cPAF-exposed slices prevented dendritic beading (Figure 6A, $n = 7$ slices from 4 animals; $P < 0.01$ vs. cPAF alone), and largely preserved LTP. Potentiation of EPSP slope appeared to be slightly blunted over the first 10 to 20 minutes following HFS but strengthened until a 2-fold potentiation was maintained after 30 minutes (Figure 6B, 2.10 ± 0.27 relative to baseline from 40 to 50 minutes; $P < 0.01$ vs. baseline and $P < 0.05$ vs. all cPAF-exposed cells).

## Discussion
We have shown that exposure to cPAF increases vulnerability to dendritic injury, including beading and spine loss that
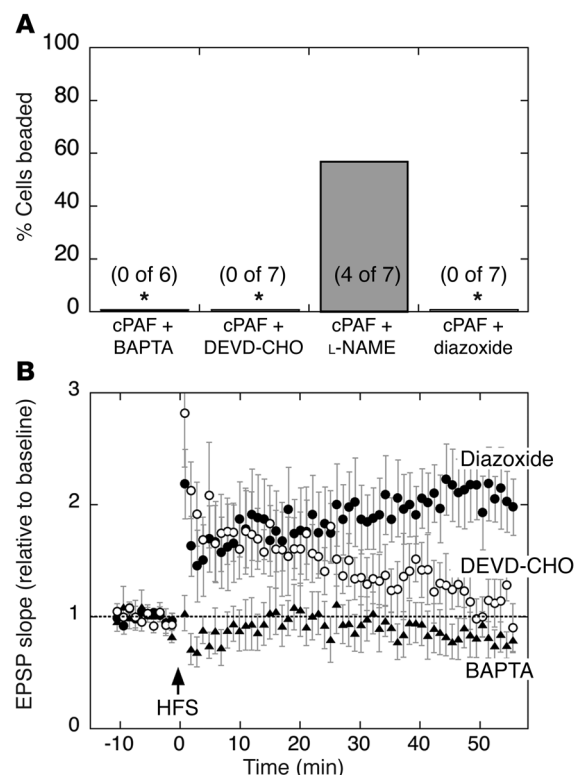
**Figure 5**
Activity-dependent dendritic beading is delayed, long lasting, and local. Dendritic beading in a cPAF-exposed hippocampal slice developed with a delay after HFS and progressed throughout the recording trial. In addition, focal swellings were restricted to discrete regions along the dendrite with no apparent disruption of dendrite and spine morphology in intervening areas. Scale bars: 20 μm.

of extracellular glutamate during acute insults such as trauma and ischemia; by transiently disrupting postsynaptic glutamate signaling, dendritic swelling may attenuate calcium-mediated excitotoxicity (17). In neuroinflammatory diseases such as HAD, on the other hand, our data suggest that dendrites may become vulnerable to localized excitotoxic damage in neighborhoods of elevated synaptic activity, which may impair function in a relatively synapse-specific manner.

Furthermore, we show that activity-dependent dendritic injury shares overlapping mechanisms with activity-dependent plasticity and suggest that interventions that prevent excitotoxic injury at the expense of LTP likely have limited utility in treatment of chronic neurodegenerative disease. Blockade of postsynaptic calcium signaling prevented dendritic beading following HFS, but because calcium is crucial for long-term plasticity (45), this did not improve synaptic function in cPAF-exposed slices (Figure 6). Likewise, caspase activity has been shown to be required for hippocampal LTP (46), and its inhibition prevented beading but failed to restore LTP. PAF-R antagonism, which inhibits LTP in some in vitro models but not in others (28, 29, 47), can impair hippocampal learning in vivo (31) and resulted in diminished LTP in our experiments; it thus may face similar limitations as a therapeutic strategy.

In contrast, pretreatment with diazoxide prevented dendritic beading while preserving LTP in cPAF-exposed slices (Figure 6). Diazoxide can precondition against insults including ischemia

and glutamate excitotoxicity (42–44) via mechanisms that include acute and delayed effects on mitochondrial calcium uptake, reactive oxygen species production, cytochrome *c* release, and prosurvival gene expression (43, 44, 48) and has long-term protective effects in a model of chronic cerebral hypoperfusion (49). Diazoxide's actions need further study, but these results nevertheless raise the possibility that chemical preconditioning may be an effective strategy for improving synaptic function during chronic neuroinflammation.

Currently, use of antagonists such as memantine to inhibit excessive NMDA receptor activation (50) is the best-studied strategy to prevent excitotoxicity while preserving synaptic function in chronic neurodegenerative disease (51). Preconditioning may represent an alternate or complementary strategy that could be especially valuable if, as our results suggest, similar patterns of NMDA receptor activation can trigger either LTP or dendritic injury, depending on the presence of inflammatory mediators.

Thus, our results demonstrate the utility of investigating dendritic beading as a potential harbinger of failure of synaptic transmission during inflammatory neurodegenerative disease. Further investigation is necessary to validate whether neuroprotective agents that can preserve synaptic plasticity compromised during dendritic beading may improve neurologic disease associated with this type of injury.

**Figure 6**
Chemical preconditioning prevents calcium- and caspase-dependent beading and restores LTP. (**A**) Rates of dendritic beading and (**B**) EPSP potentiation following high-frequency Schaffer collateral stimulation in hippocampal slices exposed to cPAF. Postsynaptic calcium chelation by intracellularly applied BAPTA eliminated dendritic beading as well as synaptic potentiation ($n = 6$). Postsynaptic inhibition of caspase-3, -6, -7, -9, and -10 by intracellular Ac-DEVD-CHO (DEVD-CHO) (10 μM) prevented dendritic beading but failed to restore a lasting potentiation ($n = 7$) while nitric oxide synthase inhibitor L-NAME had no effect on rates of dendritic beading compared with cPAF alone (Figure 4). Pretreatment with the mitochondrial $K_{ATP}$ agonist diazoxide prevented dendritic beading and restored LTP in cPAF-exposed slices (2.10 ± 0.27–fold potentiation at 40 to 50 minutes, $n = 7$). *$P < 0.01$ vs. cPAF alone (Figure 4).

## Methods

*Golgi staining and immunohistochemistry.* We studied paraformaldehyde-fixed postmortem tissue obtained from HIV-1 seropositive patients who had undergone comprehensive neuropsychological testing as previously described (52). We compared tissue from the midfrontal cortex of patients with no neuropsychological impairment ($n = 5$, postmortem interval $8 \pm 3$ hours) and from patients with HAD ($n = 5$, postmortem interval $9 \pm 2$ hours). Tissue blocks were trimmed to 2 mm³, silver-impregnated with the rapid Golgi method, and sectioned at 100 μm as previously described (7). For immunohistochemical analysis, we incubated 40-μm vibratome sections overnight with antibodies against PAF-R (1:250; Cayman Chemical Co.), detecting them with horseradish peroxidase and the Tyramide Signal Amplification-Direct (Red) system (PerkinElmer) or diaminobenzidine, followed in some studies by antibodies against MAP2 (1:100; Chemicon International) detected with FITC-conjugated horse anti-mouse IgG (1:75; Vector Laboratories). To control for nonspecific binding, we incubated PAF-R antibody overnight with a PAF-R–derived blocking peptide (1:20; Cayman Chemical Co.) prior to incubation with tissue sections. We analyzed slide-mounted sections with laser scanning confocal microscopy (MRC1024, Bio-Rad Laboratories). All sections were processed simultaneously, and experiments were repeated to assess reproducibility. Studies in patients were conducted according to the Helsinki declaration and with approval from the University of California San Diego Human Subjects Review Board. All patients provided informed consent prior to inclusion in the study and were identified by number, not name.

*Primary hippocampal cultures and dendrite imaging.* We prepared dissociated hippocampal cultures from embryonic (E18) rats as previously described (53), plated on coverslips coated with poly-D-lysine and mouse laminin (reagents from Sigma-Aldrich unless otherwise noted) in Neurobasal plus B-27 media (Gibco; Invitrogen Corp.). After 1 week, 53 mM NaCl was added (to match solutions for physiological experiments), and antioxidants were removed from the media. Experiments were repeated using cultures from multiple dissections. Care and use of animals in these experiments was approved by the University of Rochester Committee on Animal Resources and was compliant with NIH policies as well as New York state and federal statutes.

At 20–24 days in vitro, we transfected neurons with EYFP (BD Biosciences — Clontech) or mRFP-1 (kind gift of Roger Tsien, University of California San Diego, La Jolla, California, USA) vectors driven by CMV promoter in a 1:2 ratio with Lipofectamine 2000 (Invitrogen Corp.). We captured serial fluorescence images of individual, live neurons (23–30 days in vitro) before and after exposure to 130 nM cPAF (BIOMOL) and/or synaptic stimulation by KCl. For 60-hour exposure experiments, a 10 mM stock solution of cPAF (in EtOH) or vehicle was diluted into culture media. We measured neuronal survival by Hoechst nuclear staining and propidium iodide exclusion.

For acute KCl stimulation experiments, we perfused coverslips in a custom-made chamber (200 μl) with bath solution (139.5 mM NaCl, 2.5 mM KCl, 2 mM CaCl₂, 1 mM MgCl₂, 24 mM glucose, 5 mM HEPES, 0.01 mM glycine, pH 7.3) at 1 ml/min and exposed cultures to vehicle or cPAF for 20–90 minutes prior to stimulation. We locally applied KCl (90 mM) over the entire dendritic arbor of EYFP- or mRFP-expressing neurons in 3 1- or 5-second pulses (10 seconds apart) using an 8-channel drug delivery system (ALA Scientific Instruments). In some experiments we added BN52021 (BIOMOL) or CNQX and AP-5.

*Imaging and LTP in acute hippocampal slices.* We removed brains from 17- to 30-day-old male Sprague-Dawley rats anesthetized with ketamine (180 μg/g), submerged them in ice-cold solution (125 mM NaCl, 5 mM KCl, 1.25 mM NaH₂PO₄, 28 mM NaHCO₃, 0.5 mM CaCl₂, 4 mM MgCl₂, 25 mM D-glucose, 1 mM kynurenic acid, bubbled with 95% O₂/5% CO₂), and cut 250-μm

coronal slices using a vibroslice. Slices recovered in artificial cerebrospinal fluid (aCSF) (125 mM NaCl, 2.5 mM KCl, 1.25 mM NaH₂PO₄, 25 mM NaHCO₃, 2 mM CaCl₂, 1 mM MgCl₂, 25 mM D-glucose, bubbled with 95% O₂/5% CO₂) for more than 90 minutes prior to experiments.

We transferred slices to a custom-made recording chamber perfused (1 ml/min) with aCSF containing 1 μM cPAF or vehicle. We recorded membrane potentials from CA1 pyramidal neurons via whole-cell patch clamp, using 4–6 MΩ electrodes (filled with 20 mM KCl, 130 mM potassium gluconate, 0.5 mM EGTA, 10 mM HEPES, 2 mM MgS0₄, 2.5 mM ATP, 0.5 mM GTP, pH 7.3) and a Multiclamp 700A amplifier with pClamp 9 software (Axon Instruments). We stimulated afferents by constant current pulses (200 μs) via a bipolar stimulating electrode 50–200 μm away in the stratum radiatum. We included 10 μM bicuculline in the aCSF to isolate EPSPs and adjusted stimulating intensity to elicit EPSPs 30% of maximal. After more than 10 minutes of test pulses (every 15 seconds), we gave HFS (3 1-second pulses, 100 Hz trains, 20 seconds apart, at test-pulse intensity), then resumed test pulses for 50 minutes or more. In some experiments we included L-NAME, diazoxide (Alexis Biochemical Corp.), BN52021, or CV-3988 (BIOMOL) in the aCSF throughout the recording or BAPTA or Ac-DEVD-CHO in the electrode solution. We used rising EPSP slope instead of peak amplitude as an index of synaptic efficacy to avoid complication by action potentials evoked by some EPSPs after HFS. We also quantified amplitude (maximal sustained depolarization) and duration (at > 25% maximal amplitude) of depolarization during HFS.

We collected fluorescent images of dendrites from recorded cells before and after HFS, after allowing 30 μM Alexa Fluor 568 hydrazide (Invitrogen Corp.) in the recording electrode to fill the cell for more than 20 minutes. Using an external shutter to limit light exposure, we captured image frames at multiple focal planes and combined optimally focused portions of these frames to display a composite image.

*Dendrite morphology.* For in vitro experiments, we compared pre- and post-exposure images of the same cells. We considered a neuron beaded if its dendrites developed *any* focal swellings during the experiments (10, 14) though multiple dendrites were typically involved. We determined changes in spine number by counting spines on the same dendrites before and after treatment.

*Statistics.* We analyzed differences in frequencies of dendritic beading by $\chi^2$ test and changes in dendritic spine number by paired 2-tailed Student's $t$ test. We pooled EPSP slope data over 10-minute intervals and used 2-tailed Student's $t$ tests to compare between groups or time points. The significance level for all tests was set at $P < 0.05$.

Address correspondence to: Matthew J. Bellizzi, Center for Aging and Developmental Biology, University of Rochester School of Medicine and Dentistry, 601 Elmwood Avenue, Box 645, Rochester, New York 14642, USA. Phone: (585) 275-9954; Fax: (585) 276-1966; E-mail: matthew_bellizzi@urmc.rochester.edu.

1. Masliah, E., et al. 1997. Dendritic injury is a pathological substrate for human immunodeficiency virus-related cognitive disorders. HNRC Group. The HIV Neurobehavioral Research Center. *Ann. Neurol.* **42**:963–972.

2. Everall, I.P., Glass, J.D., McArthur, J., Spargo, E., and Lantos, P. 1994. Neuronal density in the superior frontal and temporal gyri does not correlate with the degree of human immunodeficiency virus-associated dementia. *Acta Neuropathol. (Berl.).* **88**:538–544.

3. Adle-Biassette, H., et al. 1999. Neuronal apoptosis does not correlate with dementia in HIV infection but is related to microglial activation and axonal damage. *Neuropathol. Appl. Neurobiol.* **25**:123–133.

4. DeKosky, S.T., and Scheff, S.W. 1990. Synapse loss in frontal cortex biopsies in Alzheimer's disease: correlation with cognitive severity. *Ann. Neurol.* **27**:457–464.

5. Terry, R.D., et al. 1991. Physical basis of cognitive alterations in Alzheimer's disease: synapse loss is the major correlate of cognitive impairment. *Ann. Neurol.* **30**:572–580.

6. Masliah, E., Ge, N., Achim, C.L., Hansen, L.A., and Wiley, C.A. 1992. Selective neuronal vulnerability in HIV encephalitis. *J. Neuropathol. Exp. Neurol.* **51**:585–593.

7. Masliah, E., et al. 1992. Cortical dendritic pathology in human immunodeficiency virus encephalitis. *Lab. Invest.* **66**:285–291.

8. Ferrer, I., Guionnet, N., Cruz-Sanchez, F., and Tunon, T. 1990. Neuronal alterations in patients with dementia: a Golgi study on biopsy samples. *Neurosci. Lett.* **114**:11–16.

9. Masliah, E., et al. 1994. Synaptic and neuritic alterations during the progression of Alzheimer's disease. *Neurosci. Lett.* **174**:67–72.

10. Park, J.S., Bateman, M.C., and Goldberg, M.P. 1996. Rapid alterations in dendrite morphology during sublethal hypoxia or glutamate receptor activation. *Neurobiol. Dis.* **3**:215–227.

11. Ivins, K.J., Bui, E.T., and Cotman, C.W. 1998. Beta-amyloid induces local neurite degeneration in cultured hippocampal neurons: evidence for neuritic apoptosis. *Neurobiol. Dis.* **5**:365–378.

12. Mattson, M.P., Keller, J.N., and Begley, J.G. 1998. Evidence for synaptic apoptosis. *Exp. Neurol.* **153**:35–48.

13. White, A.R., et al. 2001. Sublethal concentrations of prion peptide PrP106-126 or the amyloid beta peptide of Alzheimer's disease activates expression of proapoptotic markers in primary cortical neurons. *Neurobiol. Dis.* **8**:299–316.

14. Hasbani, M.J., Hyrc, K.L., Faddis, B.T., Romano, C., and Goldberg, M.P. 1998. Distinct roles for sodium, chloride, and calcium in excitotoxic dendritic injury and recovery. *Exp. Neurol.* **154**:241–258.

15. Al-Noori, S., and Swann, J.W. 2000. A role for sodium and chloride in kainic acid-induced beading of inhibitory interneuron dendrites. *Neuroscience.* **101**:337–348.

16. Hasbani, M.J., Schlief, M.L., Fisher, D.A., and Goldberg, M.P. 2001. Dendritic spines lost during glutamate receptor activation reemerge at original sites of synaptic contact. *J. Neurosci.* **21**:2393–2403.

17. Ikegaya, Y., et al. 2001. Rapid and reversible changes in dendrite morphology and synaptic efficacy following NMDA receptor activation: implication for a cellular defense against excitotoxicity. *J. Cell Sci.* **114**:4083–4093.

18. Brendza, R.P., et al. 2005. Anti-Aβ antibody treatment promotes the rapid recovery of amyloid-associated neuritic dystrophy in PDAPP transgenic mice. *J. Clin. Invest.* **115**:428–433. doi:10.1172/JCI200523269.

19. Zhu, B., Luo, L., Moore, G.R., Paty, D.W., and Cynader, M.S. 2003. Dendritic and synaptic pathology in experimental autoimmune encephalomyelitis. *Am. J. Pathol.* **162**:1639–1650.

20. Puel, J.L., Ruel, J., Gervais d'Aldin, C., and Pujol, R. 1998. Excitotoxicity and repair of cochlear synapses after noise-trauma induced hearing loss. *Neuroreport.* **9**:2109–2114.

21. Gendelman, H.E., et al. 1998. Suppression of inflammatory neurotoxins by highly active antiretroviral therapy in human immunodeficiency virus-associated dementia. *J. Infect. Dis.* **178**:1000–1007.

22. Thurnher, M.M., et al. 2000. Highly active antiretroviral therapy for patients with AIDS dementia complex: effect on MR imaging findings and clinical course. *AJNR Am. J. Neuroradiol.* **21**:670–678.

23. Genis, P., et al. 1992. Cytokines and arachidonic metabolites produced during human immunodeficiency virus (HIV)-infected macrophage-astroglia interactions: implications for the neuropathogenesis of HIV disease. *J. Exp. Med.* **176**:1703–1718.

24. Perry, S.W., et al. 1998. Platelet-activating factor receptor activation. An initiator step in HIV-1 neuropathogenesis. *J. Biol. Chem.* **273**:17660–17664.

25. Giulian, D., Vaca, K., and Noonan, C.A. 1990. Secretion of neurotoxins by mononuclear phagocytes infected with HIV-1. *Science.* **250**:1593–1596.

26. Aihara, M., Ishii, S., Kume, K., and Shimizu, T. 2000. Interaction between neurone and microglia mediated by platelet-activating factor. *Genes Cells.* **5**:397–406.

27. Clark, G.D., Happel, L.T., Zorumski, C.F., and Bazan, N.G. 1992. Enhancement of hippocampal excitatory synaptic transmission by platelet-activating factor. *Neuron.* **9**:1211–1216.

28. Wieraszko, A., Li, G., Kornecki, E., Hogan, M.V., and Ehrlich, Y.H. 1993. Long-term potentiation in the hippocampus induced by platelet-activating factor. *Neuron.* **10**:553–557.

29. Kato, K., Clark, G.D., Bazan, N.G., and Zorumski, C.F. 1994. Platelet-activating factor as a potential retrograde messenger in CA1 hippocampal long-term potentiation. *Nature.* **367**:175–179.

30. Izquierdo, I., et al. 1995. Memory enhancement by intrahippocampal, intraamygdala, or intraentorhinal infusion of platelet-activating factor measured in an inhibitory avoidance task. *Proc. Natl. Acad. Sci. U. S. A.* **92**:5047–5051.

31. Teather, L.A., Packard, M.G., and Bazan, N.G. 1998. Effects of posttraining intrahippocampal injections of platelet-activating factor and PAF antagonists on memory. *Neurobiol. Learn. Mem.* **70**:349–363.

32. Gelbard, H.A., et al. 1994. Platelet-activating factor: a candidate human immunodeficiency virus type 1-induced neurotoxin. *J. Virol.* **68**:4628–4635.

33. Lindsberg, P.J., Yue, T.L., Frerichs, K.U., Hallenbeck, J.M., and Feuerstein, G. 1990. Evidence for platelet-activating factor as a novel mediator in experimental stroke in rabbits. *Stroke.* **21**:1452–1457.

34. Kumar, R., Harvey, S.A., Kester, M., Hanahan, D.J., and Olson, M.S. 1988. Production and effects of platelet-activating factor in the rat brain. *Biochim. Biophys. Acta.* **963**:375–383.

35. Ogden, F., DeCoster, M.A., and Bazan, N.G. 1998. Recombinant plasma-type platelet-activating factor acetylhydrolase attenuates NMDA-induced hippocampal neuronal apoptosis. *J. Neurosci. Res.* **53**:677–684.

36. Xu, Y., and Tao, Y.X. 2004. Involvement of the NMDA receptor/nitric oxide signal pathway in platelet-activating factor-induced neurotoxicity. *Neuroreport.* **15**:263–266.

37. Ho, Y.S., et al. 1997. Brain acetylhydrolase that inactivates platelet-activating factor is a G-protein-like trimer. *Nature.* **385**:89–93.

38. Mori, M., et al. 1996. Predominant expression of platelet-activating factor receptor in the rat brain microglia. *J. Neurosci.* **16**:3590–3600.

39. Fitzjohn, S.M., et al. 2001. An electrophysiological characterisation of long-term potentiation in cultured dissociated hippocampal neurones. *Neuropharmacology.* **41**:693–699.

40. Patel, A.J., Lauritzen, I., Lazdunski, M., and Honore, E. 1998. Disruption of mitochondrial respiration inhibits volume-regulated anion channels and provokes neuronal cell swelling. *J. Neurosci.* **18**:3117–3123.

41. Xu, Y., et al. 2004. Targeted disruption of PSD-93 gene reduces platelet-activating factor-induced neurotoxicity in cultured cortical neurons. *Exp. Neurol.* **189**:16–24.

42. Kis, B., et al. 2003. Diazoxide induces delayed preconditioning in cultured rat cortical neurons. *J. Neurochem.* **87**:969–980.

43. Nagy, K., Kis, B., Rajapakse, N.C., Bari, F., and Busija, D.W. 2004. Diazoxide preconditioning protects against neuronal cell death by attenuation of oxidative stress upon glutamate stimulation. *J. Neurosci. Res.* **76**:697–704.

44. Domoki, F., Bari, F., Nagy, K., Busija, D.W., and Siklos, L. 2004. Diazoxide prevents mitochondrial swelling and Ca2+ accumulation in CA1 pyramidal cells after cerebral ischemia in newborn pigs. *Brain Res.* **1019**:97–104.

45. Dunwiddie, T.V., and Lynch, G. 1979. The relationship between extracellular calcium concentrations and the induction of hippocampal long-term potentiation. *Brain Res.* **169**:103–110.

46. Gulyaeva, N.V., Kudryashov, I.E., and Kudryashova, I.V. 2003. Caspase activity is essential for long-term potentiation. *J. Neurosci. Res.* **73**:853–864.

47. Kobayashi, K., et al. 1999. Platelet-activating factor receptor is not required for long-term potentiation in the hippocampal CA1 region. *Eur. J. Neurosci.* **11**:1313–1316.

48. Eliseev, R.A., Vanwinkle, B., Rosier, R.N., and Gunter, T.E. 2004. Diazoxide-mediated preconditioning against apoptosis involves activation of cAMP-response element-binding protein (CREB) and NFkappaB. *J. Biol. Chem.* **279**:46748–46754.

49. Farkas, E., et al. 2004. Diazoxide and dimethyl sulphoxide prevent cerebral hypoperfusion-related learning dysfunction and brain damage after carotid artery occlusion. *Brain Res.* **1008**:252–260.

50. Chen, H.S., et al. 1992. Open-channel block of N-methyl-D-aspartate (NMDA) responses by memantine: therapeutic advantage against NMDA receptor-mediated neurotoxicity. *J. Neurosci.* **12**:4427–4436.

51. Areosa Sastre, A., McShane, R., and Sherriff, F. 2004. Memantine for dementia. *Cochrane Database Syst. Rev.* **2004**:CD003154.

52. Cherner, M., et al. 2002. Neurocognitive dysfunction predicts postmortem findings of HIV encephalitis. *Neurology.* **59**:1563–1567.

53. Perry, S.W., Norman, J.P., Litzburg, A., and Gelbard, H.A. 2004. Antioxidants are required during the early critical period, but not later, for neuronal survival. *J. Neurosci. Res.* **78**:485–492.